Original Article
pISSN 2234-1900 · eISSN 2234-3156
Radiat Oncol J 2022;40(4):242-250
https://doi.org/10.3857/roj.2022.00332

Dosimetric evaluation of magnetic resonance imaging-guided adaptive radiation therapy in pancreatic cancer by extent of re-contouring of organs-at-risk

Jun Yeong Song[1,2], Eui Kyu Chie[1,2], Seong-Hee Kang[1], Yeon-Jun Jeon[3], Yoon-Ah Ko[3], Dong-Yun Kim[2,4], Hyun-Cheol Kang[1,2]

[1]*Department of Radiation Oncology, Seoul National University Hospital, Seoul, Korea*
[2]*Department of Radiation Oncology, Seoul National University College of Medicine, Seoul, Korea*
[3]*Seoul National University College of Medicine, Seoul, Korea*
[4]*Department of Radiation Oncology, Kyung Hee University Hospital at Gangdong, Seoul, Korea*

Received: June 13, 2022
Revised: October 31, 2022
Accepted: November 14, 2022

Correspondence:
Hyun-Cheol Kang
Department of Radiation Oncology, Seoul National University Hospital, 101 Daehak-ro, Jongno-gu, Seoul 03080, Korea.
Tel: +82-2-2072-2526
E-mail: shule@snu.ac.kr
ORCID:
https://orcid.org/0000-0002-8981-6123

Purpose: The safety of online contouring and planning for adaptive radiotherapy is unknown. This study aimed to evaluate the dosimetric difference of the organ-at-risk (OAR) according to the extent of contouring in stereotactic magnetic resonance image-guided adaptive RT (SMART) for pancreatic cancer.

Materials and Methods: We reviewed the treatment plan data used for SMART in patients with pancreatic cancer. For the online contouring and planning, OARs within 2 cm from the planning target volume (PTV) in the craniocaudal direction were re-controlled daily at the attending physician's discretion. The entire OARs were re-contoured retrospectively for data analysis. We termed the two contouring methods the Rough OAR and the Full OAR, respectively. The proportion of dose constraint violation and other dosimetric parameters was analyzed.

Results: Nineteen patients with 94 fractions of SMART were included in the analysis. The dose constraint was violated in 10.6% and 43.6% of the fractions in Rough OAR and Full OAR methods, respectively ($p = 0.075$). Patients with a large tumor, a short distance from gross tumor volume (GTV) to OAR, and a tumor in the body or tail were associated with more occult dose constraint violations—large tumor ($p = 0.027$), short distance from GTV to OAR ($p = 0.061$), tumor in body or tail ($p = 0.054$). No dose constraint violation occurred outside 2 cm from the PTV.

Conclusion: More occult dose constraint violations can be found by the Full OAR method in patients with pancreatic cancer with some clinical factors in the online re-planning for SMART. Re-contouring all the OARs would be helpful to detect occult dose constraint violations in SMART planning. Since the dosimetric profile of SMART cannot be represented by a single fraction, patient selection for the Full OAR method should be weighted between the clinical usefulness and the time and workforce required.

Keywords: Pancreatic neoplasms, Radiotherapy, Radiosurgery, Adaptation, Organs at risk

Introduction

Among hundreds of cancers, pancreatic cancer has one of the worst prognoses. The median overall survival is approximately 13–24 months in patients with localized disease and 9–16 months in locally advanced cases [1–4]. Trimodality therapy is increasingly being utilized in the setting of borderline resectable pancreatic cancer (BRPC) or locally advanced pancreatic cancer (LAPC) to improve resectability, local control, and survival [5–8]. Moreover, the PREOPANC trial investigated the oncologic outcomes of resectable pancreatic cancer (RPC) and BRPC cases who received neoadjuvant chemoradiotherapy before surgery and showed a significant survival benefit in BRPC patients [7].

Among many radiation therapy (RT) techniques, stereotactic ablative radiotherapy (SABR) offers many advantages compared to conventional fractionated RT, such as a high radiation dose [9,10], a relatively short period of treatment [11], and an excellent conformality [12]. In the SABR delivered to the pancreas, the stomach, duodenum, and bowel are considered organs-at-risk (OAR) with clinical significance. These organs are mobile and radiosensitive, posing challenges when planning RT [13,14]. One study investigated the inter-fractional motion of these OARs and showed it reaches 17 to 36 mm [13]. Stereotactic magnetic resonance image-guided adaptive radiotherapy (SMART) is a tool to overcome such concerns in SABR to a tumor surrounded by these organs. It considers the daily organ migration by re-contouring OARs. Also, real-time magnetic resonance imaging (MRI) offers a superior spatial resolution of the soft tissue of intra-abdominal organs during RT and considers the intra-fractional respiratory motion.

In the current practice of SMART to the pancreas at our institution, only a portion of the OARs close to the planning target volume (PTV) is re-contoured because OARs near the PTV are enough to produce an online adaptive plan, and its safety and reproducibility were also published to reduce the most time-consuming step of the treatment [14–16]. However, the extent of re-contouring has not been thoroughly discussed and has uncertainties. Therefore, in this study, we evaluated the dosimetric difference between the radiation plan that re-contoured the entire OARs (Full OAR) and that of the actual treatment with roughly contoured OARs (Rough OAR) in SMART.

Methods and Materials

We retrospectively reviewed the medical records and treatment plans of 19 patients who received SMART at our institution from February 2018 to May 2019. The Institutional Review Board of Seoul National University Hospital (IRB No. 2003-094-1109) approved the study and waived the requirement for informed consent. All patients were treated using the ViewRay MRIdian system (ViewRay Inc., Oakwood Village, OH, USA), which incorporates a 0.35T MRI scanner with three cobalt-60 γ-ray sources [17]. The patients were treated with preoperative, radical, and salvage aims.

The simulation process of SMART included MRI simulation with corresponding non-enhanced computed tomography (CT) simulations. Each scan was obtained in the end-expiratory phase to minimize respiratory motion. After simulation, we contoured the target volume and OARs and performed treatment planning. We defined the clinical target volume (CTV) as the pancreatic mass and its infiltration to neighboring structures. A 3–5 mm margin was expanded to all directions from the CTV to make up the PTV. The prescription dose for PTV was 40–50 Gy in 5 fractions, which was adjusted considering the relative location and distance from the surrounding OARs.

The OARs for the treatment course included the stomach, duodenum, and bowel. The institutional dose constraint policy required the V_{35} of each OAR to be less than 0.5 mL in the initial planning process. Also, in the re-optimization process for SMART, the constraint required the V_{35} of each OAR to be less than 1 mL. The UK consensus on normal tissue dose constraints for stereotactic radiotherapy [18], which was brought from the protocols of the ABC-07 and SPARC trials, was used as guidelines for the dose constraints [19,20].

All treatment plans consisted of 5 fractions of SMART. In each fraction, a daily set-up MRI was obtained using the same protocol as for the simulation. The attending physician decided whether to proceed to the treatment without making amendments to the OAR contours by comparing the anatomy between the MRI taken during the simulation and daily set-up. If the contours needed adjustment, the physician re-contoured them in real-time. For re-contouring, our institutional policy is to adjust OARs within 2 cm from the PTV in the craniocaudal direction or 3 cm, depending on the situation. Also, the attending physician decided which OARs to re-contour, considering the inter-fractional variation and proximity to the PTV. The initial plan was immediately re-optimized based on the daily contours by modifying the dose rate and beam angle.

The entire OAR was re-contoured retrospectively for every fraction of SMART regardless of the distance from the PTV (Full OAR). We contoured the duodenum from the pylorus of the stomach to the fourth portion, where it merges with the bowel. We defined the contour of the bowel as the sum of bowel loops, excluding the duodenum. It was delineated distally to the inferior aspect of the third portion of the duodenum and had no limits proximally. A representative image of the daily MR image with OAR contours using both of the contouring methods is shown in Fig. 1. Dosimetric parameters such as the maximum point dose to a volume (D_{max}), the minimal dose received by the highest irradiated volume of 1 mL (D_{1cc}), the volume receiving 35 Gy or more (V_{35}), and the volume receiving 33 Gy or more (V_{33}) were calculated. We used the same dose constraint (V_{35} < 1 mL) to evaluate the Full OAR contouring. We reviewed the dose distributions of cases that violated the dose constraint in the Full OAR contouring only.

Statistical analysis was performed using SPSS 26.0 (IBM SPSS

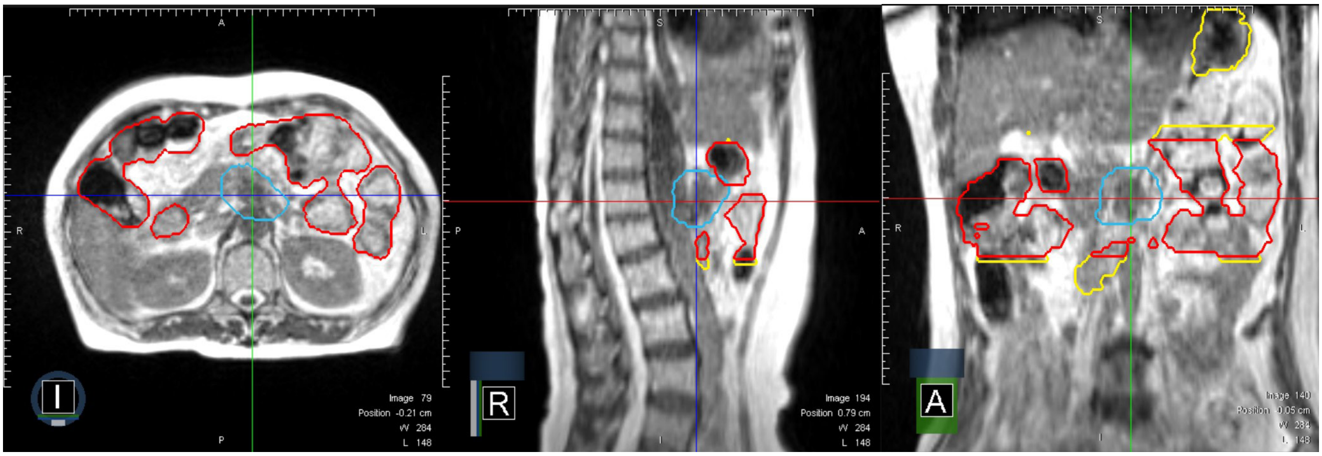

Fig. 1. MR image of OAR contours according to methods of re-contouring of one treatment fraction, with PTV (light blue) and the contours of Rough OAR (red) and Full OAR (yellow). MR, magnetic resonance; OAR, organ-at-risk; PTV, planning target volume.

Statistics for Windows; IBM Corp, Armonk, NY, USA). The chi-square test was used for comparing categorical variables, and the paired t-test was used for comparing continuous variables. A p-value of less than 0.05 was considered statistically significant. Side effects were graded according to the Common Terminology Criteria for Adverse Events v5.0 (CTCAE v5.0). Side effects assessed in grade 3 or higher were termed "severe side effects."

Results

Table 1 describes the patient and treatment characteristics. A total of 19 patients were included in the analysis. Eight patients (42.1%) had a tumor located in the uncinate process or head, and the rest had a tumor in the body or tail. The median tumor size was 3.0 cm, ranging from 2.2 to 13.2 cm. All but one patient underwent 5 fractions of adaptive radiotherapy for a total of 94 fractions. One patient received 4 fractions of RT as neoadjuvant treatment, the last fraction was skipped because the plan's quality was unacceptable, and the physician decided not to treat it after considering the risk and benefit. For every patient, we measured the distance from OARs to the gross tumor volume (GTV). The mean value was 3.5 mm, ranging from 0 to 11.9 mm. There were no patients with severe side effects related to RT.

When the three OARs were evaluated together, the dose constraint was violated in 10 fractions (10.6%), and 41 fractions (43.6%) out of 94 fractions in the Rough OAR and Full OAR methods, respectively ($p = 0.075$). Detailed descriptions of the violation of the dose constraint evaluated by individual OARs are listed in Table 2. Also, the dose distributions were reviewed in the treatment fractions where dose constraint violation was identified only in the Full OAR. Interestingly, no violation occurred outside 2 cm of the

Table 1. Patient and treatment characteristics (n = 19)

Characteristic	Value
Age (yr)	62 (46–77)
Sex	
Male	10 (52.6)
Female	9 (47.4)
Site	
Uncinate, head	8 (42.1)
Body, tail	11 (57.9)
Resectability (NCCN, 2021)	
Resectable	0 (0)
Borderline resectable	10 (52.6)
Locally advanced	6 (31.6)
Distant metastasis	3 (15.8)
Tumor size (cm)	3 (2.2–13.2)
Stage	
I–II	7 (36.8)
III–IV	12 (63.2)
Radiotherapy aim	
Preoperative	12 (63.2)
Radical	6 (36.8)
Salvage	1 (5.3)
Radiotherapy fraction	
4	1 (5.3)
5	18 (94.7)
Radiotherapy dose (Gy)	45 (42–50)
Distance from GTV to OAR (mm)	3.5
Range	0–11.9

Values are presented as number of patients (%) and median (range).
NCCN, National Comprehensive Cancer Network; GTV, gross tumor volume; OAR, organ-at-risk.

https://doi.org/10.3857/roj.2022.00332

Table 2. Dose constraint violation by OAR re-contouring method

	n	Rough OAR	Full OAR	p-value
All fractions	94	10 (10.6)	41 (43.6)	0.075
Resectability				
Borderline resectable	49	5 (10.2)	27 (55.1)	0.033
Locally advanced	30	5 (16.7)	8 (26.7)	0.460
Distant metastasis	15	0 (0.0)	6 (40.0)	N/A
GTV to OAR distance (mm)				
≥ 5	25	1 (4.0)	8 (32.0)	0.484
< 5	69	9 (13.0)	33 (47.8)	0.054
Site				
Uncinate, head	39	4 (10.3)	15 (38.5)	0.617
Body, tail	55	6 (10.9)	26 (47.3)	0.061
Tumor size, pre-RT (cm)				
≥ 2	35	5 (14.3)	19 (54.3)	0.027
< 2	59	5 (8.5)	22 (37.3)	0.896
Stage group				
I, II	35	5 (14.3)	16 (45.7)	0.008
III, IV	59	5 (8.5)	25 (42.4)	0.911

Values are presented as number of patients (%).
OAR, organ-at-risk; GTV, gross tumor volume; RT, radiotherapy.

Table 3. Mean value of V_{35} by OAR re-contouring method in subgroups

Subgroup	n	Rough OAR		Full OAR		p-value
		V_{35} (mL)	95% CI	V_{35} (mL)	95% CI	
All patients	94	0.748	0–9.50	2.101	0–18.31	< 0.001
'Tumor size ≥ 2 cm' and 'GTV to OAR distance < 5 mm'	43	1.030	0–9.50	2.211	0–16.43	0.063
'Tumor size ≥ 2 cm' and 'Tumor site body & tail'	25	0.398	0–1.27	1.488	0–7.75	0.017
'GTV to OAR distance < 5 mm' and 'Tumor site body & tail'	44	0.510	0–1.59	1.994	0–7.75	< 0.001

OAR, organ-at-risk; GTV, gross tumor volume; V_{35}, volume receiving 35 Gy or more; CI, confidence interval.

PTV.

In addition, various clinicopathologic factors were analyzed, and BRPC ($p = 0.023$), tumor size of 2 cm or more ($p = 0.027$), and stage group I or II ($p = 0.008$) were associated with a higher proportion of dose constraint violation in Full OAR. Similarly, other factors such as a distance from GTV to OAR of less than 5 mm ($p = 0.061$) and primary tumor in the body and tail ($p = 0.054$) were associated with a higher proportion of dose constraint violations in Full OAR with marginal significance.

After considering the clinical context and applicability, tumor size, distance from GTV to OAR, and primary tumor site were chosen as factors for the subgroup analysis. Analyses were performed by dividing the factors into subgroups grouped by two of the three factors and comparing the V_{35} of each subgroup. The V_{35} was used in place of dose constraint violation to evaluate the dosimetric difference more comprehensively with a continuous variable. The results are shown in Table 3. For all patients, the mean value of the V_{35} (mL) for Rough OAR and Full OAR showed a significant difference with 0.748 and 2.101, respectively ($p < 0.001$). A difference in the V_{35} was consistently seen across the subgroups. Except for a marginally significant difference demonstrated in the subgroup grouped by tumor size and distance from GTV to OAR ($p = 0.063$).

Other dosimetric parameters, including dose constraint, were investigated for the individual OARs. For each OAR, the differences of dose constraint violations, D_{max}, D_{1cc}, V_{35}, and V_{33} between two contouring methods were investigated (Table 4). In the duodenum, there were no violated fractions in the Rough OAR method, but in the Full OAR, 13% of the fractions violated the dose constraint. This trend was consistent with the other dosimetric parameters—D_{max} ($p < 0.001$), D_{1cc} ($p = 0.009$), V_{35} ($p = 0.040$), V_{33} ($p = 0.039$). However, the violated fraction in the stomach was 10.3% in the Rough OAR method and 16.1% in the Full OAR method, showing no statistically significant difference ($p = 0.597$). Other dosimetric parameters did not show any significant difference—D_{max} (p =

Table 4. Comparison of dosimetric parameters calculated by using each re-contouring method

	n	Rough OAR	Full OAR	p-value
All OARs				
Violated fractions	94	10 (10.6)	41 (43.6)	0.075
D_{max} (Gy)		35.21 ± 7.81	37.73 ± 7.73	< 0.001
D_{1cc} (Gy)	30	5 (16.7)	12 (40.0)	0.009
V_{35} (mL)	59	5 (8.5)	25 (42.4)	0.04
V_{33} (mL)	5	0 (0)	4 (80.0)	0.039
Duodenum				
Violated fractions	92	0 (0)	12 (13.0)	N/A
D_{max} (Gy)		35.21 ± 7.81	37.73 ± 7.73	< 0.001
D_{1cc} (Gy)		28.87 ± 6.13	30.08 ± 6.40	0.009
V_{35} (mL)		0.22 ± 0.26	0.60 ± 1.80	0.04
V_{33} (mL)		0.57 ± 0.52	1.02 ± 2.22	0.039
Stomach				
Violated fractions	87	9 (10.3)	14 (16.1)	0.597
D_{max} (Gy)		35.07 ± 10.36	34.98 ± 9.84	0.949
D_{1cc} (Gy)		30.44 ± 9.40	29.37 ± 9.43	0.393
V_{35} (mL)		0.55 ± 1.52	0.66 ± 1.42	0.628
V_{33} (mL)		1.16 ± 1.81	1.30 ± 2.08	0.629
Small bowel				
Violated fractions	67	1 (1.5)	19 (28.4)	0.109
D_{max} (Gy)		36.64 ± 4.62	38.98 ± 7.11	0.006
D_{1cc} (Gy)		31.63 ± 4.75	32.28 ± 5.89	0.077
V_{35} (mL)		0.31 ± 0.31	1.50 ± 2.95	< 0.001
V_{33} (mL)		1.12 ± 0.90	2.57 ± 4.14	< 0.001

Values are presented as number (%) or mean ± standard deviation.
OAR, organ-at-risk; D_{max}, maximum point dose to an organ or tumor target; D_{1cc}, minimal dose received by the highest irradiated volume of 1 mL; V_{33}, volume receiving 33 Gy or more; V_{35}, volume receiving 35 Gy or more; N/A, not applicable.

0.949), D_{1cc} ($p = 0.393$), V_{35} ($p = 0.628$), V_{33} ($p = 0.629$). In the bowel, there was no significant difference in the proportion of violated fractions between the OAR contouring methods ($p = 0.109$), but other dose-volume parameters indicated larger volume or higher dose in the Full OAR method—D_{max} ($p = 0.006$), V_{35} ($p < 0.001$), V_{33} ($p < 0.001$). To summarize, the V_{35} of each OAR and overall OARs are depicted as a box-and-whisker plot in Fig. 2. Also, a representative image of the contours of Rough OAR and Full OAR of a SMART fraction that had substantial discrepancy of V_{35} is depicted in Fig. 3: maximum V_{35} of individual OARs in Rough OAR (0.24 mL) and Full OAR (9.54 mL).

Discussion and Conclusion

In SMART, daily re-contouring of the OARs provides an accurate evaluation of the intra-abdominal OARs, in which significant inter- and intra-fractional variability exist. To the best of our knowledge, this is the first study to investigate the safety of SMART for pancreatic cancer by comparing different extents of OAR re-contouring. An ideal method to evaluate dose distribution would be to draw Full OARs for all patients. However, in practice, issues such as time constraints and patient compliance (i.e., unable to maintain a supine position) are challenging. Accordingly, this study evaluated the dosimetric difference between the two distinct OAR contouring methods and investigated which patient population differed using Full OAR contouring. We could find some significant clinical factors that can be used for patient selection for the time-consuming procedure, such as tumor size, stage, distance from the GTV to OAR, and tumor location. The dosimetric difference was evident in the subgroups defined by two of the factors listed and suggested patient subgroups that could benefit from the extensive re-contouring. Regarding the individual OARs, the dosimetric parameters did not differ significantly between contouring methods for the stomach. However, there were significant differences in the duodenum and bowel. Therefore, for patients with the risk factors described above, the duodenum and bowel rather than the stomach could benefit from Full OAR contouring.

In reviewing the dose distribution of the cases that violated the

https://doi.org/10.3857/roj.2022.00332

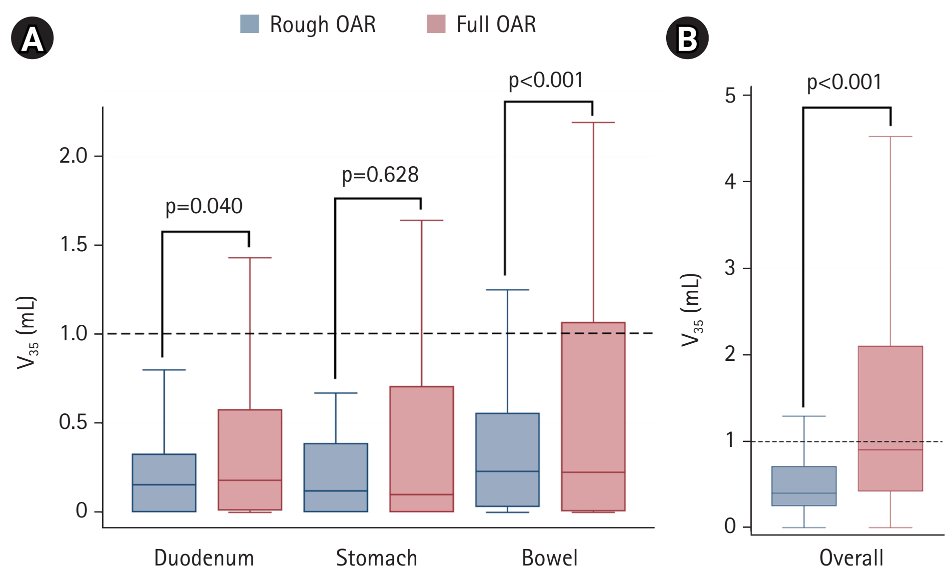

Fig. 2. Box-and-whisker plots showing values of V_{35} (mL) of individual OARs (A) and maximum V_{35} values of overall OARs (B) for all the adaptive fractions according to contouring methods. V_{35}, volume receiving 35 Gy or more; OAR, organ-at-risk.

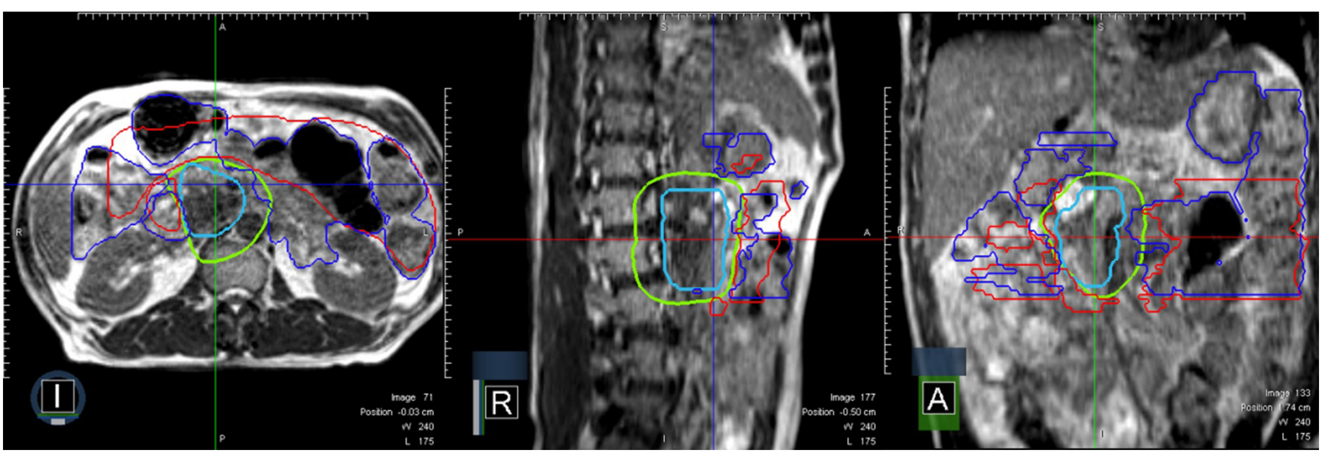

Fig. 3. MR image of OAR contours according to methods of re-contouring of one treatment fraction Showing V_{35} discrepancy, with PTV (light blue) and the contours of Rough OAR (red), Full OAR (blue) and isodose line of 35 Gy (light green). MR, magnetic resonance; OAR, organ-at-risk; PTV, planning target volume; V_{35}, volume receiving 35 Gy or more.

dose constraint in the Full OAR, but not in the Rough OAR, we found that violations were located solely within 2 cm from the PTV contour. This indicates that the additional detection of dose constraints in the Full OAR were not due to the delineation of the contours outside the 2 cm distance from the PTV, but could rather be attributed to the re-contouring of all of the OARs, regardless of the physician's decision. The sparing of the areas outside the 2 cm distance from the PTV is due to the co-planar technique and the steep dose gradient of SABR planning system, making delivery of high dose to remote areas unlikely [21,22]. Although these violations did not result in severe RT-related side effects, constant efforts in re-contouring the OARs could benefit in accurately evaluating the dose distribution, detecting dose constraint violation and re-planning according to the dose distribution.

We evaluated the dosimetric profiles for each fraction. Ten of 94 fractions (10.6%) showed a violation of dose constraints, even in the Rough OAR. However, one SMART course is usually made up of 5 fractions, and a dose constraint violation in a single fraction does not necessarily result in a violation for the whole treatment course. Areas that received the highest level of radiation may differ throughout the treatment course. Thus, there may not have been a violation in terms of the entire course. Daily anatomic variations of the OAR should be considered to make an accurate evaluation of the accumulated dose of the treatment course. Dose accumulation of all the fractions using deformable image registration (DIR) would be helpful. Bohoudi et al. [23] reported a study of DIR-based dose accumulation in prostate cancer treated with SMART. The authors showed that $V_{20Gy-32Gy}$ from the total accumulated dose delivered to the bladder rather than the dose of each fraction correlates well with the patient's symptom score. In the pancreas, a similar approach as in this study could be used to evaluate the dosimetric profile of the entire treatment course and to find a potential surrogate index associated with dosimetry of the total treatment or the incidence of adverse events.

Recently, auto-segmentation for OARs using deep learning for RT has gained attention in the field, and techniques are evolving [24–26]. Although challenging, many studies deal with auto-segmentation in intra-abdominal organs, and they report non-inferior results compared with expert-drawn contours [27,28]. These studies are based on cone-beam CT images, but studies from other organs such as the prostate employ MRI-based auto-segmentation [29]. Although this method is not mature enough to apply to daily practice, if applied to SMART, it would reduce re-contouring from the most time-consuming step to a few seconds and needs constant attention.

The current study's analysis is based on our institution's dose constraint (V_{35} < 1 mL). Thus, when we apply a different dose constraint, it would alter the proportions of the violation. Several published dose tolerance guidelines for abdominal OARs exist for 5 fraction-SABR, each employing various dose parameter [30–33]. Also, the cutoffs of the constraint vary widely. For instance, the cutoff of D_{max} ranges from 30 Gy to 45 Gy [33–37]. The reason why this discrepancy occurs is that the dose constraint is drawn from normal tissue complication probability (NTCP) models, which are derived from separate datasets of complications after RT [15,38,39]. Furthermore, there is evidence that the NTCP can vary according to the irradiated volume [40], use of chemotherapeutic agents [41], and fractionation schemes [42]. Thus, a dose constraint should be chosen accordingly to the patient and tumor setting and tailored individually.

This study had several limitations. First, this study was designed as a retrospective review and contains the inherent potential for selection bias. To minimize selection bias, we included 19 consecutive patients without further selection. Secondly, the Rough OARs were occasionally omitted for some OARs under the judgement of the attending physician, thus hindering clear comparison between the two distinct re-contouring methods. Third, to apply the results of the current study to clinical practice, clinical evidence with a high level of relevance is needed for the dose constraint of SMART. We could generate more solid factors associated with OAR contouring from the prospective data with a larger number of patients. In addition, as mentioned above, the dose constraint violation from a single fraction does not necessarily translate to a violation of the total treatment. Therefore, it is ambiguous to interpret dose constraint violations concerning clinical adverse events. No severe side effects were observed among the patients in the study, even in the group with a violation. Therefore, further analysis of dose constraint violation using DIR-based dose accumulation is warranted. Moreover, the clinical significance of dose constraint violation should be clarified by assessing how many adverse events occur.

In conclusion, Full OAR differed in the proportion of violated fractions from the Rough OAR in SMART for pancreatic cancer. Patient groups with a large tumor, a short distance from the OAR to GTV, and a tumor in the body or tail showed benefit in further discriminating occult dose constraint violations and should be considered for Full OAR contours, especially in the duodenum and bowel. Also, delineating all of the OARs within 2 cm from the PTV, rather than outside 2 cm from the PTV, would help to discover occult violations. However, it should be weighted between the clinical usefulness and its cost as the dosimetric profile of SMART cannot be represented by a single fraction.

Statement of Ethics

The Institutional Review Board of Seoul National University Hospital (IRB No. 2003-094-1109) approved the study and waived the requirement for informed consent.

Conflict of Interest

No potential conflict of interest relevant to this article was reported.

Funding

None.

Author Contribution

Conceptualization: HCK, YJJ, YAK, JYS; Investigation and methodology: HCK, YJJ, YAK, SHK, JYS; Project administration: EKC, HCK; Resources: EKC, SHK, HCK; Supervision: HCK; Writing of the original draft: YJJ, YAK, JYS; Writing of the review and editing, JYS, HCK; Software: SHK; Validation: SHK, JYS; Formal analysis: JYS; Data curation: YJJ, YAK, JYS; Visualization: YJJ, YAK, JYS. SHK. All the authors have proofread the final version.

https://doi.org/10.3857/roj.2022.00332

Data Availability Statement

The data that support the findings of this study are available from the corresponding author upon reasonable request.

References

1. Regine WF, Winter KA, Abrams R, et al. Fluorouracil-based chemoradiation with either gemcitabine or fluorouracil chemotherapy after resection of pancreatic adenocarcinoma: 5-year analysis of the U.S. Intergroup/RTOG 9704 phase III trial. Ann Surg Oncol 2011;18:1319–26.
2. Van Laethem JL, Hammel P, Mornex F, et al. Adjuvant gemcitabine alone versus gemcitabine-based chemoradiotherapy after curative resection for pancreatic cancer: a randomized EORTC-40013-22012/FFCD-9203/GERCOR phase II study. J Clin Oncol 2010;28:4450–6.
3. Loehrer PJ Sr, Feng Y, Cardenes H, et al. Gemcitabine alone versus gemcitabine plus radiotherapy in patients with locally advanced pancreatic cancer: an Eastern Cooperative Oncology Group trial. J Clin Oncol 2011;29:4105–12.
4. Hammel P, Huguet F, van Laethem JL, et al. Effect of chemoradiotherapy vs chemotherapy on survival in patients with locally advanced pancreatic cancer controlled after 4 months of gemcitabine with or without erlotinib: the LAP07 Randomized Clinical Trial. JAMA 2016;315:1844–53.
5. Chuong MD, Springett GM, Freilich JM, et al. Stereotactic body radiation therapy for locally advanced and borderline resectable pancreatic cancer is effective and well tolerated. Int J Radiat Oncol Biol Phys 2013;86:516–22.
6. Quan K, Sutera P, Xu K, et al. Results of a prospective phase 2 clinical trial of induction gemcitabine/capecitabine followed by stereotactic ablative radiation therapy in borderline resectable or locally advanced pancreatic adenocarcinoma. Pract Radiat Oncol 2018;8:95–106.
7. Versteijne E, Suker M, Groothuis K, et al. Preoperative chemoradiotherapy versus immediate surgery for resectable and borderline resectable pancreatic cancer: results of the Dutch Randomized Phase III PREOPANC Trial. J Clin Oncol 2020;38:1763–73.
8. Jang JY, Han Y, Lee H, et al. Oncological benefits of neoadjuvant chemoradiation with gemcitabine versus upfront surgery in patients with borderline resectable pancreatic cancer: a prospective, randomized, open-label, multicenter phase 2/3 trial. Ann Surg 2018;268:215–22.
9. Rudra S, Jiang N, Rosenberg SA, et al. Using adaptive magnetic resonance image-guided radiation therapy for treatment of inoperable pancreatic cancer. Cancer Med 2019;8:2123–32.
10. Toesca DA, Ahmed F, Kashyap M, et al. Intensified systemic therapy and stereotactic ablative radiotherapy dose for patients with unresectable pancreatic adenocarcinoma. Radiother Oncol 2020;152:63–9.
11. Jung J, Yoon SM, Park JH, et al. Stereotactic body radiation therapy for locally advanced pancreatic cancer. PLoS One 2019;14:e0214970.
12. Ermongkonchai T, Khor R, Muralidharan V, et al. Stereotactic radiotherapy and the potential role of magnetic resonance-guided adaptive techniques for pancreatic cancer. World J Gastroenterol 2022;28:745–54.
13. Palacios MA, Bohoudi O, Bruynzeel AM, et al. Role of daily plan adaptation in MR-guided stereotactic ablative radiation therapy for adrenal metastases. Int J Radiat Oncol Biol Phys 2018;102:426–33.
14. Bohoudi O, Bruynzeel AM, Senan S, et al. Fast and robust online adaptive planning in stereotactic MR-guided adaptive radiation therapy (SMART) for pancreatic cancer. Radiother Oncol 2017;125:439–44.
15. Murphy JD, Christman-Skieller C, Kim J, Dieterich S, Chang DT, Koong AC. A dosimetric model of duodenal toxicity after stereotactic body radiotherapy for pancreatic cancer. Int J Radiat Oncol Biol Phys 2010;78:1420–6.
16. Lamb J, Cao M, Kishan A, et al. Online adaptive radiation therapy: implementation of a new process of care. Cureus 2017;9:e1618.
17. Mutic S, Dempsey JF. The ViewRay system: magnetic resonance-guided and controlled radiotherapy. Semin Radiat Oncol 2014;24:196–9.
18. Hanna GG, Murray L, Patel R, et al. UK consensus on normal tissue dose constraints for stereotactic radiotherapy. Clin Oncol (R Coll Radiol) 2018;30:5–14.
19. Holyoake DL, Robinson M, Silva M, et al. SPARC, a phase-I trial of pre-operative, margin intensified, stereotactic body radiation therapy for pancreatic cancer. Radiother Oncol 2021;155:278–84.
20. Cancer Research UK. A trial looking at stereotactic body radiotherapy and chemotherapy for people with locally advanced bile duct cancer (ABC-07) [Internet]. London, UK: Cancer Research UK; 2022 [cited 2022 Nov 20]. Available from: https://www.cancerresearchuk.org/about-cancer/find-a-clinical-trial/a-trial-looking-chemotherapy-stereotactic-radiotherapy-people-locally-advanced-bile-duct-cancer-abc-07.
21. Gayen S, Kombathula SH, Manna S, Varshney S, Pareek P. Dosimetric comparison of coplanar and non-coplanar volumetric-modulated arc therapy in head and neck cancer treated with radiotherapy. Radiat Oncol J 2020;38:138–47.
22. Amsbaugh MJ, Woo SY. Stereotactic radiation therapy tech-

niques. In : Halperin EC, Brady LW, Wazer DE, Perez CA, editors. Perez & Brady's principles and practice of radiation oncology. 7th ed. Philadelphia, PA: Lippincott Williams & Wilkins; 2019, p. 436–47.

23. Bohoudi O, Bruynzeel AM, Tetar S, Slotman BJ, Palacios MA, Lagerwaard FJ. Dose accumulation for personalized stereotactic MR-guided adaptive radiation therapy in prostate cancer. Radiother Oncol 2021;157:197–202.
24. Cardenas CE, Yang J, Anderson BM, Court LE, Brock KB. Advances in auto-segmentation. Semin Radiat Oncol 2019;29:185–97.
25. Cha E, Elguindi S, Onochie I, et al. Clinical implementation of deep learning contour autosegmentation for prostate radiotherapy. Radiother Oncol 2021;159:1–7.
26. Byun HK, Chang JS, Choi MS, et al. Evaluation of deep learning-based autosegmentation in breast cancer radiotherapy. Radiat Oncol 2021;16:203.
27. Dai X, Lei Y, Wynne J, et al. Synthetic CT-aided multiorgan segmentation for CBCT-guided adaptive pancreatic radiotherapy. Med Phys 2021;48:7063–73.
28. Liu Y, Lei Y, Wang T, et al. CBCT-based synthetic CT generation using deep-attention cycleGAN for pancreatic adaptive radiotherapy. Med Phys 2020;47:2472–83.
29. Pathmanathan AU, van As NJ, Kerkmeijer LG, et al. Magnetic resonance imaging-guided adaptive radiation therapy: a "Game Changer" for prostate treatment? Int J Radiat Oncol Biol Phys 2018;100:361–73.
30. Wulf J, Haedinger U, Oppitz U, Thiele W, Mueller G, Flentje M. Stereotactic radiotherapy for primary lung cancer and pulmonary metastases: a noninvasive treatment approach in medically inoperable patients. Int J Radiat Oncol Biol Phys 2004;60:186–96.
31. Molinelli S, de Pooter J, Mendez Romero A, et al. Simultaneous tumour dose escalation and liver sparing in stereotactic body radiation therapy (SBRT) for liver tumours due to CTV-to-PTV margin reduction. Radiother Oncol 2008;87:432–8.
32. Oermann EK, Slack RS, Hanscom HN, et al. A pilot study of intensity modulated radiation therapy with hypofractionated stereotactic body radiation therapy (SBRT) boost in the treatment of intermediate- to high-risk prostate cancer. Technol Cancer Res Treat 2010;9:453–62.
33. Timmerman RD. An overview of hypofractionation and introduction to this issue of seminars in radiation oncology. Semin Radiat Oncol 2008;18(4):215–22.
34. Bae SH, Kim MS, Cho CK, et al. Predictor of severe gastroduodenal toxicity after stereotactic body radiotherapy for abdominopelvic malignancies. Int J Radiat Oncol Biol Phys 2012;84:e469–74.
35. Barney BM, Olivier KR, Macdonald OK, Fong de Los Santos LE, Miller RC, Haddock MG. Clinical outcomes and dosimetric considerations using stereotactic body radiotherapy for abdominopelvic tumors. Am J Clin Oncol 2012;35:537–42.
36. Barney BM, Markovic SN, Laack NN, et al. Increased bowel toxicity in patients treated with a vascular endothelial growth factor inhibitor (VEGFI) after stereotactic body radiation therapy (SBRT). Int J Radiat Oncol Biol Phys 2013;87:73–80.
37. Marks LB, Yorke ED, Jackson A, et al. Use of normal tissue complication probability models in the clinic. Int J Radiat Oncol Biol Phys 2010;76(3 Suppl):S10–9.
38. Rouvalis P. Cryogenic surgery of the prostate and cystostomy using a trocar under local anesthesia in high risk patients. Z Urol Nephrol 1971;64:231–4.
39. Goldsmith C, Price P, Cross T, Loughlin S, Cowley I, Plowman N. Dose-volume histogram analysis of stereotactic body radiotherapy treatment of pancreatic cancer: a focus on duodenal dose constraints. Semin Radiat Oncol 2016;26:149–56.
40. Hoyer M, Roed H, Sengelov L, et al. Phase-II study on stereotactic radiotherapy of locally advanced pancreatic carcinoma. Radiother Oncol 2005;76:48–53.
41. de Lange SM, van Groeningen CJ, Meijer OW, et al. Gemcitabine-radiotherapy in patients with locally advanced pancreatic cancer. Eur J Cancer 2002;38:1212–7.
42. Park C, Papiez L, Zhang S, Story M, Timmerman RD. Universal survival curve and single fraction equivalent dose: useful tools in understanding potency of ablative radiotherapy. Int J Radiat Oncol Biol Phys 2008;70:847–52.

https://doi.org/10.3857/roj.2022.00332